Soluble SorCS1 binds the insulin receptor to enhance insulin sensitivity.

Mads Kjolby[1,2,3*#], Peter Breining[1,2,3*], Karen Marie Pedersen[1,3], Niels Wellner[1,3], Karen Marie Juul Sørensen[1,3,4], Anette Marianne Prior Gjesing[5], Dovile Januliene[4,8], Dorthe Maria Vittrup[3], Arulmani Manavalan[6], Maarten Rotman[6], Gangadaar Thotakura[6], Guido Hermey[7], Peder Madsen[3], Christian B. Vaegter[3], Søren Thirup[4], Olof Asplund[9], Rashmi B. Prasad[9], Edwin T. Parlevliet[10], Patrick C.N. Rensen[10], Andreas Nygaard Madsen[11], Birgitte Holst[11], Olav M. Andersen[1,3], Arne Möller[4,8], Torben Hansen[5], Anders Nykjaer[1,3,6#].

[1]PROMEMO and DANDRITE, Aarhus University, Denmark; [2]Department of Clinical Pharmacology, Aarhus University Hospital, Denmark and Danish Diabetes Academy; [3]Department of Biomedicine, Aarhus University, Denmark; [4]Department of Molecular Biology, Aarhus University; [5]Novo Nordisk Foundation Center for Basic Metabolic Research, Copenhagen University, Denmark; [6]Department of Neuroscience, Mayo Clinic, Florida, USA; [7]Institute for Molecular and Cellular Cognition, Center for Molecular Neurobiology Hamburg, University Medical Center Hamburg-Eppendorf; [8]Osnabrück University, Frankfurt Am Main Area, Germany; [9]Lund University Diabetes Centre, Malmö, Sweden; [10]Dept. Medicine, Div. Endocrinology, and Einthoven Laboratory for Experimental Vascular Medicine, Leiden University Medical Center (LUMC), Leiden, The Netherlands; [11]RMPC, Department of Biomedical Sciences, Copenhagen University, Denmark;

* Shared first authors. #Corresponding authors

Anders Nykjaer
PROMEMO and DANDRITE
Department of Biomedicine
Hoegh-Guldbergsgade 10,
Aarhus University
DK-8000 Aarhus C
Denmark
Phone: +45 2899 2384
Email:an@biomed.au.dk

Mads Kjolby
DANDRITE
Department of Biomedicine,
Hoegh-Guldbergsgade 10,
Aarhus University
DK-8000 Aarhus C
Denmark
Phone: +45 6086 6653
Kjolby@biomed.au.dk

Word count: 2511 words, including abstract (150), but excluding title, authors, figure legends and references.

Type 2 diabetes has reached endemic proportions and is a substantial burden for the affected patients and the society. Along with lifestyle factors, a number of genetic loci predisposing to type 2 diabetes have been identified, including *SORCS1* that encodes the transmembrane receptor SorCS1. The ectodomain of SorCS1 (sol-SorCS1) is shed from plasma membranes but the biological function of this fragment is unknown. Here we show that sol-SorCS1 acts as a high-affinity binding partner for the insulin receptor to stabilize the receptor and increase insulin affinity, protein kinase B activation, and glucose uptake in myocytes. Sol-SorCS1 is liberated from adipocytes, and in diabetic patients the plasma concentration positively correlates with body mass index, but inversely with plasma glucose. In mouse models of insulin resistance, exogenous sol-SorCS1 restored insulin sensitivity. We conclude that sol-SorCS1 increases peripheral insulin sensitivity and propose sol-SorCS1 as a novel insulin sensitizing adipokine and potential antidiabetic agent.

13 The mechanisms controlling insulin sensitivity and glucose metabolism are fundamental to all
14 vertebrates. Insulin resistance is an early hallmark for the development of type 2 diabetes[1,2] as insulin
15 sensitivity and peripheral tissue glucose uptake is essential to acutely buffer plasma glucose. The
16 downstream signaling pathways of the insulin receptor (IR) in skeletal muscle are well described[3].
17 Among the second messengers, the most prominent pathway regulating the insertion of GLUT4-
18 containing vesicles is the protein kinase B (AKT) signaling cascade[3]. However, whether this pathway
19 can be dynamically regulated through interaction with co-receptors or other membrane proteins is
20 unknown[4-6]. The existence of a molecular thermostat to adapt insulin sensitivity to the metabolic state
21 would transform our conceptual understanding on how key metabolic processes can be controlled.

22 SorCS1 is a member of the Vps10p-domain family of sorting receptors that also comprises
23 sortilin, SorLA, SorCS2, and SorCS3[7-10]. Several studies have identified *SORCS1* as a susceptibility
24 locus for type 2 diabetes mellitus that is conserved between humans[11-13], rats[14] and mice[15]. Recently,
25 intracellular SorCS1 was shown to facilitate the biogenesis of insulin containing secretory granules, but
26 a function outside the β-cells was not studied[16]. We therefore performed RNA sequencing on human
27 samples focusing on major peripheral tissues involved in glucose homeostasis (**Fig 1,a**). Notably, we
28 found that SorCS1 expression was highest in adipose tissue surpassing that of the pancreatic islets
29 whereas expression in the liver was hardly detected. We previously showed that every hour up to 95%
30 of SorCS1 (sol-SorCS1) is liberated from the plasma membrane by ADAM17/TACE mediated cleavage
31 but the biological relevance of this observation is unknown[17,18]. Given that human and murine adipose
32 tissue express ADAM17/TACE[17], we examined, whether body mass index (BMI) associates with the
33 plasma concentration of sol-SorCS1. To this end we assessed the correlation between BMI and the
34 concentration of sol-SorCS1 in plasma in a cohort of diabetic patients and healthy controls. We found

35 that sol-SorCS1 positively correlated with BMI and most prominently did so in the diabetic cohort (**Fig**
36 **1,b**). Accordingly, sol-SorCS1 could be liberated from human adipocytes as it was clearly detected in
37 the conditioned medium from human subcutaneous adipose tissue explants (**Fig. 1,c**). By
38 immunoprecipitation (IP) we also detected SorCS1 expression in lysates of visceral fat from mice and
39 differentiated murine 3T3-L1 adipocytes, respectively (**Fig. 1,d-e**). Notably, the conditioned medium of
40 the 3T3-L1 cultures was enriched in the soluble form of SorCS1 that migrated slightly faster than the
41 full-length receptor present in the corresponding lysate. Although SorCS1 protein was found in the
42 myocyte-derived murine cell line C2C12 (**Extended data 1,a**), we failed to detect the soluble receptor
43 in the conditioned media (**Extended data 1,b**). We next examined whether sol-SorCS1 levels is
44 associated with plasma glucose. Remarkably, among the diabetic patients sol-SorCS1 inversely
45 correlated with plasma glucose (**β**-value -2.6E-3, P<0.001) (**Fig 1,f**), suggesting that the soluble receptor
46 may impact glucose metabolism.

47 We hypothesized that sol-SorCS1 could serve as an adipose tissue derived peptide hormone
48 to compensate for an increase in BMI by lowering plasma glucose levels and preventing hyperglycemia.
49 To test this hypothesis, we sought to assess a potential glycemic regulatory function of the soluble
50 receptor. We therefore injected an adenovirus encoding human sol-SorCS1 (AV-sol-SorCS1) or AV-
51 LacZ (encoding β-galactosidase), as a negative control, into the tail vein of diet-induced obese
52 (39.5±1.2g) hyperglycemic C57BL/6 mice (DIO mice). Eleven days after viral transduction,
53 overexpression of the soluble receptor substantially mitigated the diabetic phenotype by lowering both
54 the elevated plasma glucose and insulin levels corresponding to a 24% decrease in plasma glucose and a
55 22% reduction in insulin levels, respectively (**Fig 2,a-b**). To test the antidiabetic efficacy of sol-SorCS1
56 in another and more severe diabetic model, we turned to the leptin receptor knockout mouse model
57 (*db/db*) that rapidly develops progressive obesity and type 2 diabetes. One week after injection with AV-

58 LacZ, plasma glucose was increased by 55% and insulin by 65% due to the gradual worsening of the
59 diabetic phenotype (**Fig. 2,c-d**). Remarkably, following AV-sol-SorCS1 treatment plasma glucose
60 remained unchanged and this despite a decrease in plasma insulin levels, indicating increased insulin
61 sensitivity. In the intraperitoneal glucose tolerance test (IPGTT), AV-sol-SorCS1 mice responded
62 markedly stronger with lower plasma glucose levels at all timepoints corresponding to a reduction in the
63 area under the curve (AUC) by 79.5% (**Fig. 2,e-f)**. The treated animals also exhibited superior ability in
64 mobilizing insulin compared to the control group, revealing a spare capacity of insulin production that
65 the control animals did not possess (**Fig. 2g)**. Notably, regardless the level of sol-SorCS1 overexpression
66 we never observed any signs of hypoglycemia due to a compensatory decrease in insulin secretion.

67 Next, we performed hyperinsulinemic euglycemic clamp[19,20] which is commonly used to
68 assess glucose deposition rates and insulin sensitivity. With the mice clamped to their basal fasting
69 glucose levels (**Fig. 2,h**), the necessary glucose infusion rate to maintain stable plasma glucose levels in
70 AV-sol-SorCS1 mice was substantially higher compared to the AV-LacZ group (**Fig. 2,i**). Notably, sol-
71 SorCS1 increased peripheral glucose uptake by 41%, demonstrating that sol-SorCS1 greatly increases
72 insulin sensitivity in peripheral tissues (**Fig. 2,j**). The difference in severity of diabetes progression was
73 further emphasized when measuring glycated hemoglobin (HbA1c) three weeks after viral injection in
74 another set of mice (**Fig 2,k**). In the AV-LacZ group, HbA1c had increased considerably whereas it was
75 only marginally higher in the AV-sol-SorCS1 group, indicating a long-lasting beneficial effect of the
76 soluble receptor in reducing plasma glucose.

77 We previously reported that in neurons, the SorCS1 paralogues sortilin and SorCS2, can
78 physically interact through their extracellular domains with the tropomyosin receptor kinase B (TrkB)
79 that binds brain-derived neurotrophic factor (BDNF), to enable its signaling capacity[21,22]. We
80 hypothesized that SorCS1 may likewise engage a tyrosine kinase receptor to promote its activity. Given

81 the genetic association with type 2 diabetes and its glucose lowering function, we asked whether this
82 tyrosine kinase receptor could be the insulin receptor. To assess this, we first performed co-IP
83 experiments between SorCS1 and IR in transfected HEK293 cells in the absence or presence of insulin
84 (**Fig. 3,a**). Antibodies against IR co-precipitated SorCS1 and vice versa, and this interaction was
85 unaffected by preincubation with 100 nM insulin, a concentration that saturates IR. Next, we evaluated
86 the affinity of the receptor-receptor interaction by surface plasmon resonance (SPR) analysis using the
87 extracellular domains of SorCS1, corresponding to sol-SorCS1, and the extracellular domain of IR. We
88 found that sol-SorCS1 bound immobilized IR with an estimated affinity of 5 nM (**Fig. 3,b**). Importantly,
89 the interaction between SorCS1 and IR was not prevented by insulin, as the signals for binding of SorCS1
90 and insulin to IR separately were additive when the two ligands were co-injected (**Fig. 3,c**). Since insulin
91 did not bind to immobilized SorCS1 (**Extended Data 2)**, the combined data indicate that IR can form a
92 trimeric complex with insulin and soluble SorCS1. Pro-insulin, glucagon, or glucagon-like peptide 1
93 (GLP-1) also did not bind to immobilized SorCS1 (**Extended Data 2**). We then asked whether full-length
94 SorCS1, when embedded in plasma membrane, may regulate insulin binding to IR and its signaling
95 capacity. First, we overexpressed IR in HEK293 cells (HEK-IR) alone or in combination with SorCS1-
96 b, an isoform of SorCS1 that predominates at the plasma membrane[18]. Remarkably, SorCS1 increased
97 the affinity of insulin to IR by approximately five-fold (**Fig. 3,d**). Given that overexpression of SorCS1
98 and IR could potentially result in ligand independent autoactivation, we compared insulin signaling in
99 C2C12 cells with or without CRISPR/Cas9 mediated knockout of *Sorcs1*. The most prominent pathway
100 regulating the insertion of GLUT4 containing vesicles is the AKT signaling cascade. Indeed, we found
101 that SorCS1-deficient C2C12 cells were substantially less insulin responsive than control cells as the
102 EC_{50} for pAKT was left-shifted approximately five-fold (**Fig. 3,e and Extended Data 1,b**). Together the
103 data suggested that the glucose lowering effect of SorCS1 is accounted for by an allosteric change in IR

104 that increases its insulin binding affinity, leading to stronger AKT signaling. To substantiate such a
105 model, we measured the thermal stability of full-length IR in the absence or presence of sol-SorCS1
106 using a cellular thermal shift assay (CETSA)[23]. We found that incubation with sol-SorCS1 right-shifted
107 the melting curve of IR in overexpressing HEK293 cells corresponding to an increase in Tm from 47.8°C
108 to 49.5°C (**Fig 3,f**). The data suggests that sol-SorCS1 induces a conformational change in IR, and
109 supports that allosteric changes in IR may be accountable for the beneficial effects of SorCS1 on insulin
110 binding and signaling.

111 We previously reported that SorCS1 exists as a monomer and as a non-covalent dimer, with
112 the oligomeric state, being regulated by the level of glycosylation[24]. However, the functional implications
113 of the two forms, e.g. whether the relative amounts of the two forms dictate binding specificity remains
114 unknown. To explore the spatial distribution of the monomer and dimer at the subcellular level, we used
115 a bimolecular fluorescence complementation (BiFC) assay[25]. HEK-IR cells were transfected with two
116 human SorCS1 constructs each containing one-half of the Venus fluorescent protein. When SorCS1
117 dimerizes the two Venus fragments unite to elicit a green fluorescent signal that echoes the subcellular
118 distribution of dimeric SorCS1. First, we stained the cells with an antibody that recognizes both
119 monomeric and dimeric SorCS1 and found monomeric SorCS1 is present at the plasma membrane
120 whereas the BiFC-positive signal representing dimeric SorCS1 is restricted to intracellular compartments
121 (**Fig. 4,a**). This is in accordance with our previous observation demonstrating that through its maturation,
122 N-linked oligosaccharides transforms SorCS1 from the dimeric form into the monomeric configuration[24].
123 Binding of insulin to the IR changes its dimeric and symmetric conformation to adapt an asymmetric
124 configuration (personal communication, Dr Poul Nissen, manuscript to be resubmitted). This prompted
125 us to study whether the interaction of IR is restricted to the monomeric form of SorCS1. To demonstrate
126 that monomeric SorCS1 and IR can interact, we first combined the BiFC signal with proximity ligation

127 assay (PLA) for the two receptors. In this assay a red fluorescent signal appears when SorCS1 and IR are
128 in close proximity (<40 nm). We observed a strong PLA signal at the plasma membrane that was BiFC-
129 negative, indicating that only monomeric SorCS1 binds IR, which suggest that the biologically active
130 form of SorCS1 is the monomer (**Fig. 4,b).** To substantiate this hypothesis, we produced an adenovirus
131 encoding a truncated version of SorCS1 that is unable to dimerize and studied its biological activity.
132 SorCS1 harbors a consensus sequence (amino acids 695 to 702) for cleavage by prohormone convertases
133 of the subtilisin/Kex2-like family, such as furin[26]. Truncation at this site gives rise to a soluble fragment
134 of roughly 60 kDa (aa130-695 after cleavage of the propeptide and signal peptide) that comprises the
135 entire Vps10p domain but does not possess the dimerization site (**Extended Data 3)**. We overexpressed
136 this explicit monomer by adenovirus (AV-aa1-695-SorCS1) and compared its glucose lowering capacity
137 to AV-sol-SorCS1 (aa1-1097) that comprises the entire ectodomain and likely represents a mixture of
138 monomer and dimer. At day 7 and 14 after viral injection both soluble SorCS1 variants were equally
139 potent in reducing plasma glucose (**Fig. 4,c**). This finding indicates that shed monomeric sol-SorCS1
140 plays an important role in the biological effects on peripheral glucose disposal.

141 To demonstrate that the beneficial properties of sol-SorCS1 was not secondary to
142 intrahepatic effects upon hepatic overexpression and to clearly isolate the actions of monomeric from
143 dimeric sol-SorCS1, we studied the glucose lowering effect of the two species upon exogenous
144 administration. In practice, the two forms were purified by size exclusion chromatography from medium
145 of cells expressing sol-SorCS1 and the two species injected intraperitoneally into *db/db* mice at 10 hrs
146 and 1 hr prior to a glucose tolerance test. Intriguingly, monomeric sol-SorCS1 profoundly improved
147 glucose tolerance whereas the dimeric version showed no effect on glucose disposal (**Fig. 4,d**). The AUC
148 for plasma glucose in the glucose tolerance test was reduced by approximately 60% (from 1060 to 393
149 mM*min, $P<0.05$) in animals treated with monomeric sol-SorCS1 (**Fig. 4,e**).

150 Aimed at demonstrating a direct effect of monomeric sol-SorCS1 on muscle cells, we
151 developed a real time *in vitro* assay with a 1 minute resolution in cellular glucose-uptake (**Fig. 4,f-g,**
152 **Extended Data 4**)[27]. Applying this highly sensitive real-time assay on primary murine myotubes,
153 revealed that sol-SorCS1 does not function as an insulin mimetic, since preincubation with either variant
154 of sol-SorCS1 for 20 minutes did not increase uptake of the glucose analogue (**Extended Data 4,b**).
155 Subjecting naïve myotubes to 10 nM insulin had no effect on glucose analogue uptake. However, after
156 preincubation with 100 nM monomeric sol-SorCS1 addition of 10 nM insulin led to a 45% increase in
157 glucose uptake rate (**Fig 4,h-i**). In marked contrast, 10 nM insulin stimulation after preincubation with
158 dimeric sol-SorCS1 which showed no such effect. However, addition of 100 nM insulin to naïve or
159 dimeric sol-SorCS1 treated myotubes increased glucose uptake to match the rate obtained for myotubes
160 stimulated with 10 nM insulin and pretreated with the sol-SorCS1 monomer (**Extended data 4,c).** Hence,
161 monomeric sol-SorCS1 acts directly on myotubes to enhance their insulin sensitivity and induces a rapid
162 increase in glucose uptake.
163 In conclusion, we have demonstrated that SorCS1 circulates in plasma in a soluble form
164 that can be produced by adipose tissue. Once secreted it acts as a hormone that targets tissues remote
165 from its site of production to increase insulin sensitivity**.** Accordingly, overexpression of the soluble
166 receptor fragment reduces plasma glucose and insulin levels in mice with diet induced obesity and limits
167 diabetes progression in leptin receptor knockout mice. We provide evidence that the biological activity
168 of sol-SorCS1 is restricted to its monomeric form and suggest that once liberated from the plasma
169 membrane it acts in an endocrine fashion (**Extended Data Fig. 5).** Our study nominates sol-SorCS1 as
170 a novel adipokine to control peripheral glucose metabolism and insulin sensitivity, and as a template for
171 future anti-diabetic drug development.
172

Acknowledgements

The study was funded by the Lundbeck Foundation grant no. R248-2017-431 (AN), DANDRITE-R248-2016-2518 (AN), R90-2011-7723 (AN); The Independent Research Fund Denmark grant no. DFF-7016-00261 (AN); The Novo Nordisk Foundation grant no. NNF16OC0020984 (AN); The Danish National Research Foundation grant no. DNRF133 (AN); The Danish Diabetes Academy, Novo Nordisk Foundation (MK), Lundbeck Foundation Emerge (MFK, AN). We thank Benedicte Vestergaard, Anja Aagaard and Anne Kerstine Thomassen for excellent technical assistance and Professor Alan Attie, University Wisconsin-Madison, WI, for insightful discussion.

Figure 1

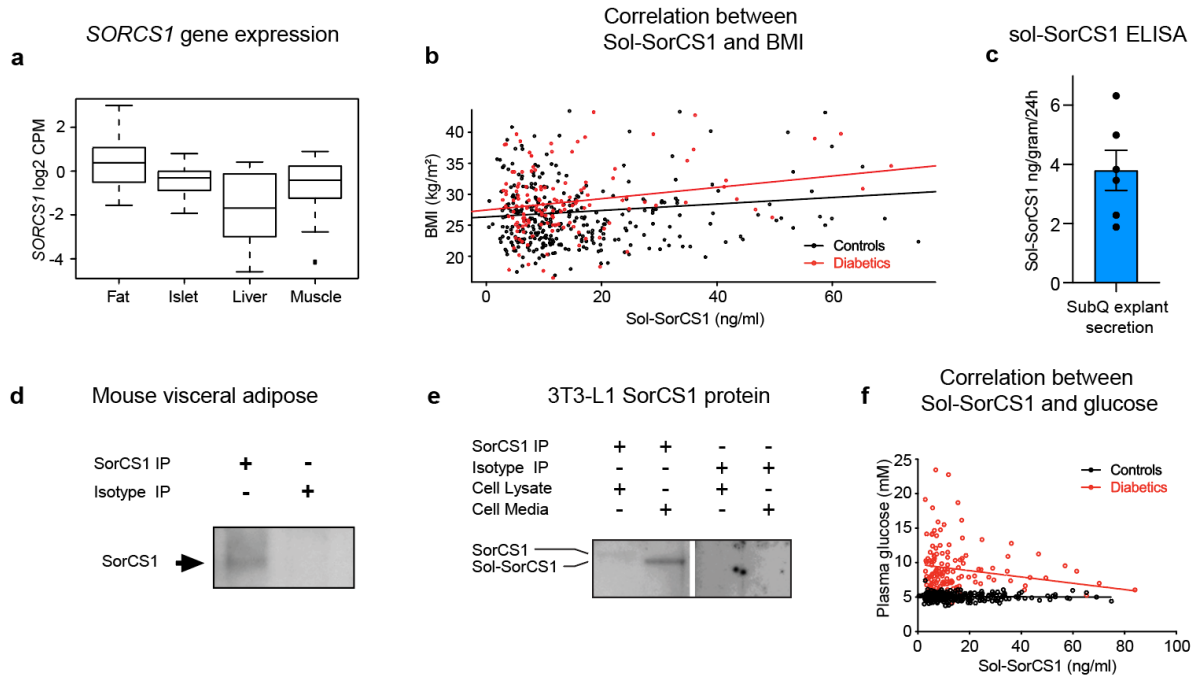

Figure 1: SorCS1 is expressed in, and secreted from, adipose tissue

a, mRNA expression of *SORCS1* in human tissues (n=12/group). **b**, in a group of healthy controls and diabetes patients (n=328 and n=124, resp.) plasma levels of sol-SorCS1 positively correlate with BMI (**β**-value 0.011, P=0.007 and **β**-value 0.058, P<0.05, respectively). **c,** Sol-SorCS1 ELISA of media from 24h incubation of human subcutaneous adipose tissue (SubQ) explants (3.80±0.68 ng/gram/24h). **d**, protein immunoblot of murine SorCS1 in adipose tissue. **e**, full-length SorCS1 and its soluble shed form in 3T3-L1 adipocytes. **f**, in the human cohort sol-SorCS1 negatively correlates with fasting plasma glucose (**β**-value -2.6E-3, P<0.001).

Figure 2

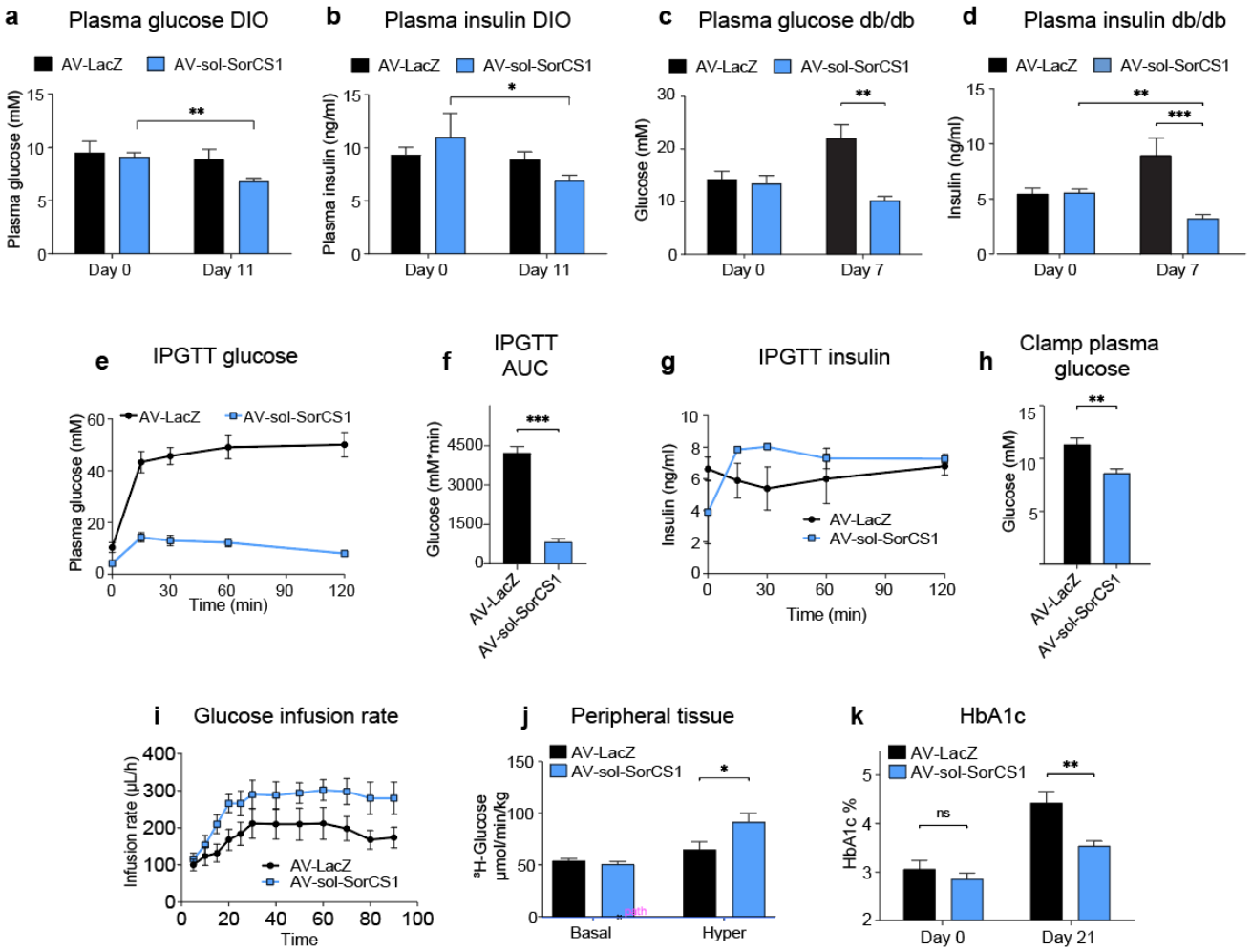

Figure 2: Sol-SorCS1 is an insulin sensitizer.

a-d, treatment with AV-sol-SorCS1, but not AV-LacZ, reduces plasma glucose levels and plasma insulin in 16 weeks old diet-induced-obese (DIO) mice and in 7 weeks old *db/db* mice. **e**, enhanced glucose uptake determined by IPGTT in AV-sol-SorCS1 treated *db/db* mice shown in real-time and, **f**, as AUC (n=4/group). **g**, plasma insulin in the IPGTT shown in e-h. **h**, lower initial fasting plasma glucose in AV-sol-SorCS1 treated *db/db* mice but higher infusion rate during euglycemic hyperinsulinemic clamp, **i**

199 (n=5/group). **j**, the higher infusion rate is accounted for by increased peripheral glucose uptake (primarily

200 muscle tissue). **k**, reduced HbA1c in *db/db* mice 21 days after infection with AV-sol-SorCS1 infection.

201 Data are presented as means ± SEM, * = $P<0.05$, ** = $P<0.01$, *** = $P<0.001$.

202

203

204

205 Figure 3

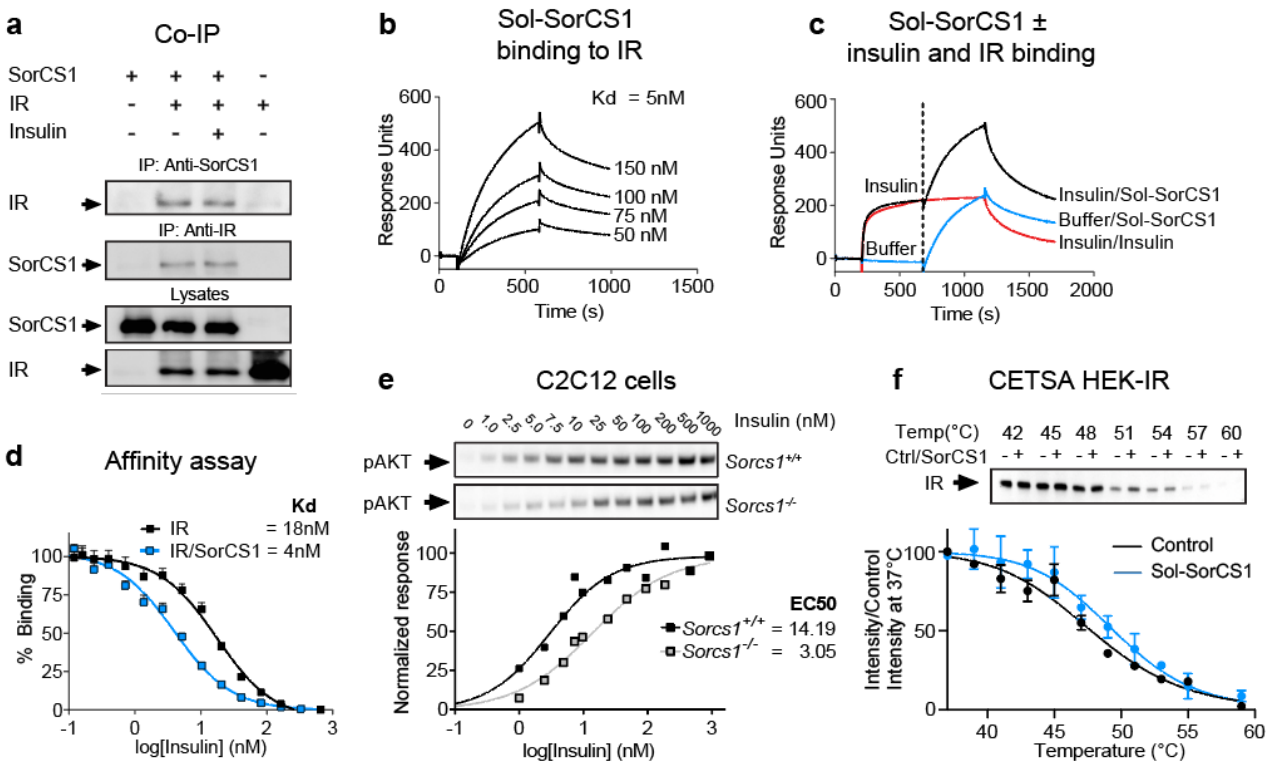

206

207

208 **Figure 3:** SorCS1 and IR physically interact.

209 **a**, Co-immunoprecipitation between SorCS1 and proIR/IR. The interaction is independent of the
210 presence of saturating concentrations of insulin (100 nM). **b**, SPR analysis demonstrates dose-dependent
211 binding of sol-SorCS1 to IR. **c**, Complex formation of SorCS1, IR, and insulin determined by SPR. At
212 1200 sec, the additive signals for Sol-SorCS1 (*blue*) and insulin (*red*) equals the response units obtained
213 when IR is incubated with both proteins simultaneously (*black*). **d**, SorCS1 overexpression in HEK293
214 cells increases insulin affinity to IR. **e**, Reduced phosphorylation of AKT in *Sorcs1*$^{-/-}$ C2C12 cells. **f**, 5
215 min. incubation with 1 µM sol-SorCS1 increases thermal stability of IR from HEK-IR lysate (n=3).

216

217 Figure 4

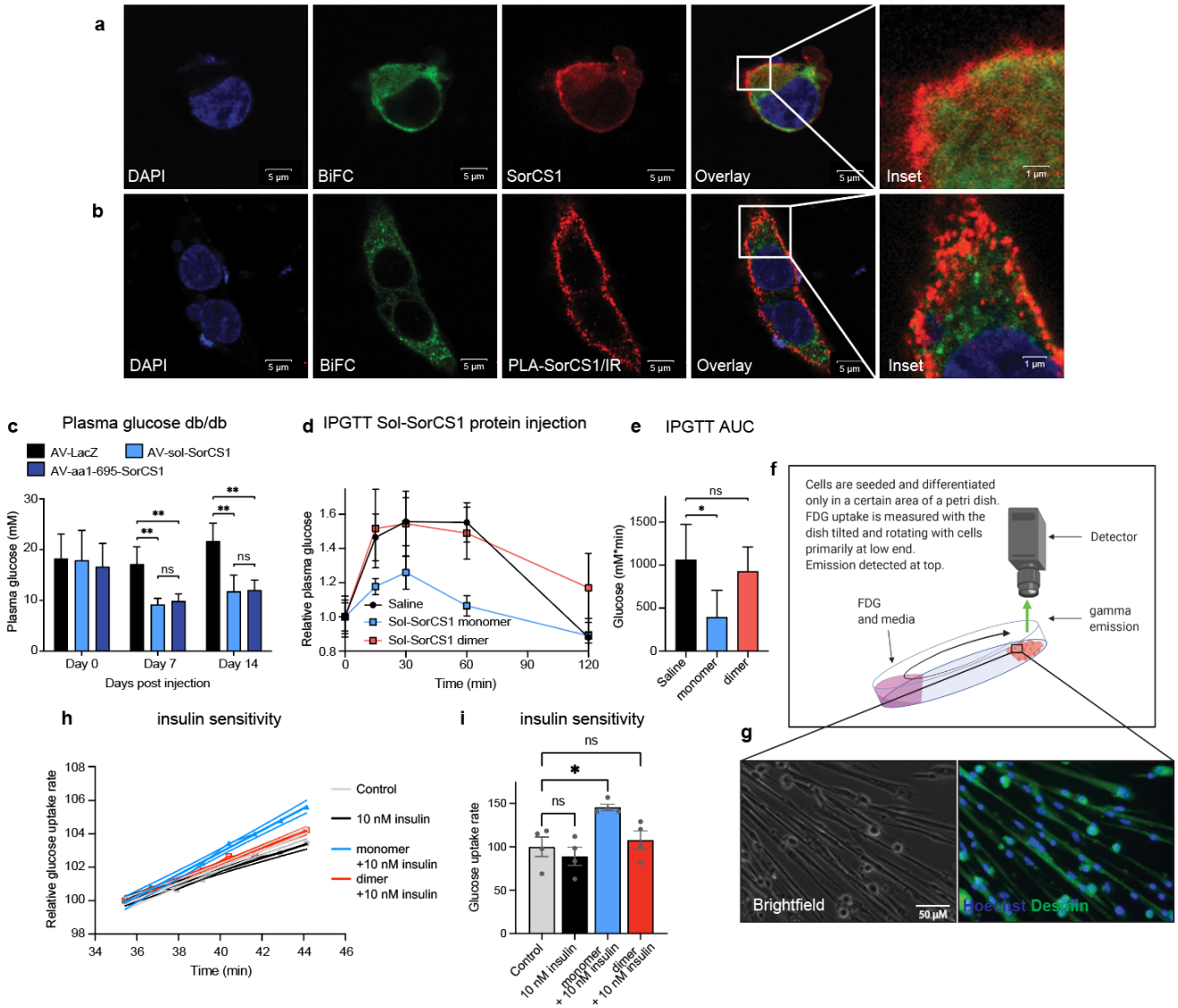

218

219 **Figure 4:**

220 **A,** SorCS1 dimers that are BiFC-positive (*green*) are confined to cytosolic compartments, whereas
221 monomeric and BiFC-negative SorCS1 (*red*), is present at the cell surface (**a**, *inset*). **b**, in non-
222 permeabilized HEK293, PLA for SorCS1 and IR (*red*) demonstrates binding between monomeric
223 SorCS1 (BiFC-negative) and IR. **c**, AV-sol-SorCS1 and AV-aa1-695-SorCS1, but not AV-LacZ, reduces
224 plasma glucose in 8 weeks old *db/db* mice. **d**, intraperitoneal injection of recombinant monomeric, but

225 not dimeric, sol-SorCS1 increases glucose clearance in *db/db* mice. **e**, AUC of the data displayed in panel
226 **d**. **f**, illustration of kinetic FDG uptake assay. **g**, representative brightfield and fluorescence image of the
227 murine myotubes used for the uptake study. Hoechst in *blue* and Desmin in *green*. **h**, relative FDG uptake
228 in control cells (gray), 10 nM insulin (black), sol-SorCS1 monomer 10 + nM insulin (blue) and sol-
229 SorCS1 dimer 10 + nM insulin (red) (n=4). **i**, bar chart overview of the slopes displayed in panel **h**.
230 statistics are done on actual slopes. Data are presented as means ± SEM, * = $P<0.05$, ** = $P<0.01$.
231
232
233
234

235 Extended data figure 1

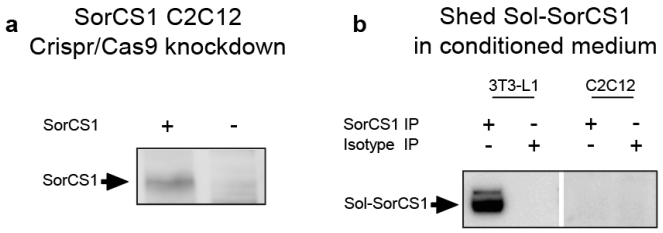

236

237

238 **Extended Data Figure 1:**

239 **a**, Through Crisp-Cas9 gene editing, we created a stable SorCS1 knockdown model of the murine C2C12

240 muscle cell line. SorCS1 protein presence was validated in the wild-type cells by western blotting using

241 a single homemade polyclonal antibody targeting murine SorCS1 (MK-S1). **b,** SorCS1 could not be

242 detected in serum free conditioned medium (hybridoma) from C2C12 cells using two polyclonal

243 antibodies, whereas it was clearly present in conditioned medium from 3T3-L1.

244
245

246 Extended data figure 2

247

Sol-SorCS1 or IR binding

	Sol-SorCS1	Insulin Receptor
Insulin	No binding	Kd - 9 nM
Pro-Insulin	No binding	Kd - 330 nM
GLP1	No binding	Not determined
Glucagon	No binding	Not determined

248

249 **Extended Data Figure 2:**

250 Table showing no binding between sol-SorCS1 and various key factors in peripheral plasma glucose

251 clearance.

252
253

254 Extended data figure 3

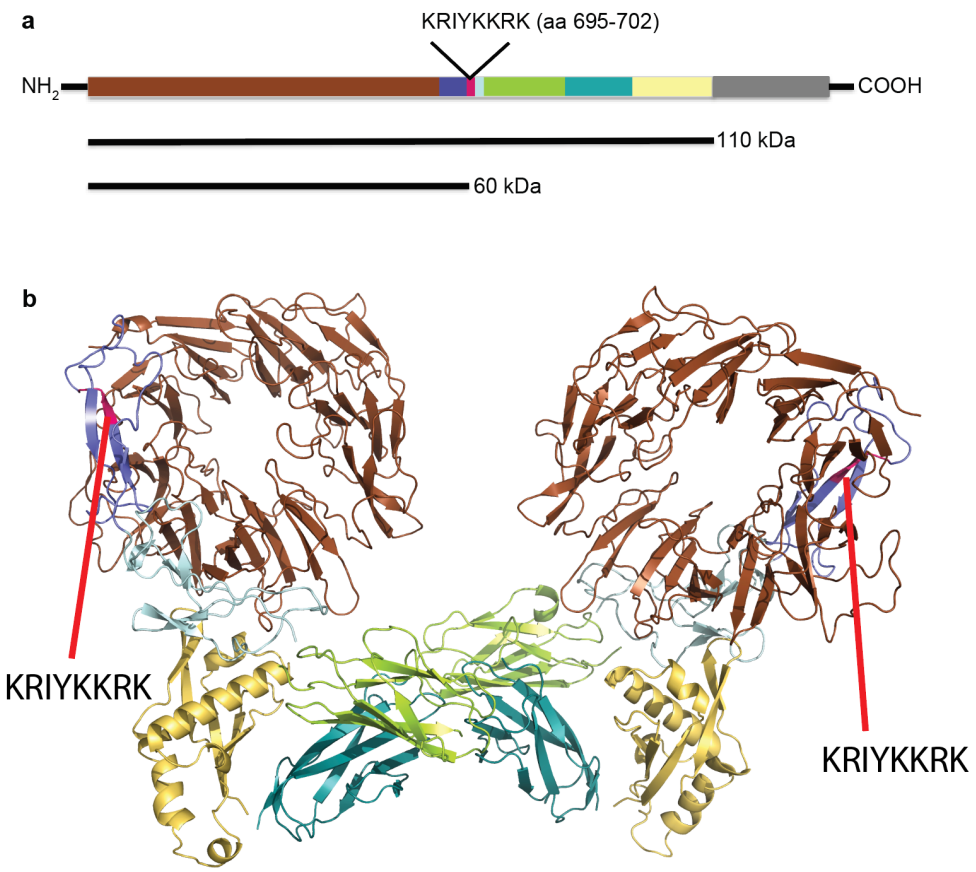

255

256 **Extended Data Figure 3:**

257 **a**, illustration of potential furin site on SorCS1 in dimer formation and the termination site of the explicit
258 monomer "aa1-695-sol-SorCS1". **b**, A homology model of human dimeric SorCS1 based on murine
259 SorCS2 (PDB entry 6FG9)[28] constructed using the SwissModel service[29]. The individual domains were
260 manually overlaid on the single particle reconstructed envelope of monomeric SorCS1 (EMDB entry
261 EMD-3708)[24]. The SorCS1 dimer: Colors: β-propeller – *brown*, 10CCa – *blue*, 10CCb – *lightblue*, PKD1
262 – *green*, PKD2 – *cyan*, and SoMP – *yellow*. The position of the putative furin site (699-KKRK-702)
263 delimiting the sol 1-702-SorCS1 construct is indicated in pink.

264 Extended data figure 4

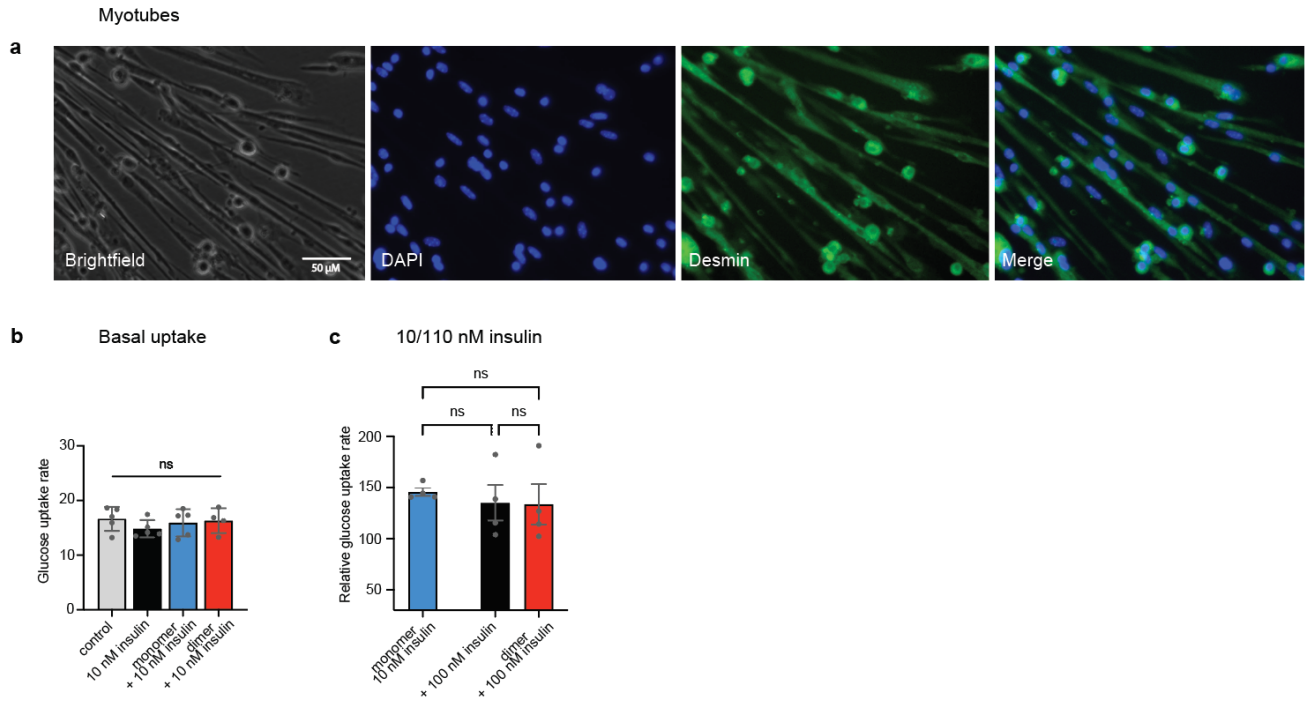

265

266 **Extended Data Figure 4:**

267 **a**, All individual panels from brightfield and fluorescence image Fig 4,h. **b**, Basal glucose analogue
268 uptake rate showing no difference between interventions on each study day. **c**, naïve myotubes and
269 myotubes pretreated with 100 nM dimeric sol-SorCS1 increase glucose analogue uptake only when
270 stimulated with an additional 100 nM insulin compared to 10 nM insulin in myotubes pretreated with
271 100 nM monomeric sol-SorCS1.

272 Extended data figure 5

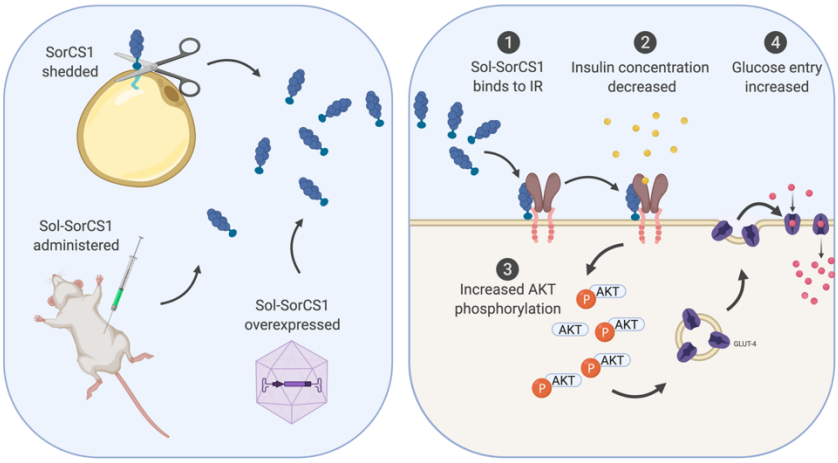

273

274 **Extended Data Figure 5:** An illustrated summery of mode of action of sol-SorCS1.

275 The illustration shows how shedding, injection or overexpression of sol-SorCS1 leads to increased

276 glucose uptake through increased insulin receptor signaling while circulating insulin concentrations

277 decrease implying increased receptor sensitivity.

278 **References:**

279 1. Shanik, M.H., *et al.* Insulin resistance and hyperinsulinemia: is hyperinsulinemia the cart or the
280 horse? *Diabetes Care* **31 Suppl 2**, S262-268 (2008).
281 2. Warram, J.H., Martin, B.C., Krolewski, A.S., Soeldner, J.S. & Kahn, C.R. Slow glucose
282 removal rate and hyperinsulinemia precede the development of type II diabetes in the offspring
283 of diabetic parents. *Ann Intern Med* **113**, 909-915 (1990).
284 3. Boucher, J., Kleinridders, A. & Kahn, C.R. Insulin Receptor Signaling in Normal and Insulin-
285 Resistant States. *Cold Spring Harbor Perspectives in Biology* **6**, a009191-a009191 (2014).
286 4. Kim, S.J., *et al.* mTOR complex 2 regulates proper turnover of insulin receptor substrate-1 via
287 the ubiquitin ligase subunit Fbw8. *Mol Cell* **48**, 875-887 (2012).
288 5. Tremblay, F., *et al.* Identification of IRS-1 Ser-1101 as a target of S6K1 in nutrient- and
289 obesity-induced insulin resistance. *Proc Natl Acad Sci U S A* **104**, 14056-14061 (2007).
290 6. Blagosklonny, M.V. TOR-centric view on insulin resistance and diabetic complications:
291 perspective for endocrinologists and gerontologists. *Cell Death Dis* **4**, e964 (2013).
292 7. Willnow, T.E., Petersen, C.M. & Nykjaer, A. VPS10P-domain receptors - regulators of
293 neuronal viability and function. *Nat Rev Neurosci* **9**, 899-909 (2008).
294 8. Willnow, T.E., Kjolby, M. & Nykjaer, A. Sortilins: new players in lipoprotein metabolism.
295 *Curr Opin Lipidol* **22**, 79-85 (2011).
296 9. Kjolby, M., *et al.* Sort1, encoded by the cardiovascular risk locus 1p13.3, is a regulator of
297 hepatic lipoprotein export. *Cell Metab* **12**, 213-223 (2010).
298 10. Goettsch, C., Kjolby, M. & Aikawa, E. Sortilin and Its Multiple Roles in Cardiovascular and
299 Metabolic Diseases. *Arterioscler Thromb Vasc Biol* **38**, 19-25 (2018).
300 11. He, Y., Fang, Z. & Yu, G. Sortilin-related VPS10 domain containing receptor 1 and
301 Alzheimer's disease-associated allelic variations preferentially exist in female or type 2 diabetes
302 mellitus patients in southern Han Chinese. *Psychogeriatrics* **12**, 215-225 (2012).
303 12. Paterson, A.D., *et al.* A genome-wide association study identifies a novel major locus for
304 glycemic control in type 1 diabetes, as measured by both A1C and glucose. *Diabetes* **59**, 539-
305 549 (2010).
306 13. Goodarzi, M.O., *et al.* SORCS1: a novel human type 2 diabetes susceptibility gene suggested
307 by the mouse. *Diabetes* **56**, 1922-1929 (2007).
308 14. Granhall, C., Park, H.B., Fakhrai-Rad, H. & Luthman, H. High-resolution quantitative trait
309 locus analysis reveals multiple diabetes susceptibility loci mapped to intervals<800 kb in the
310 species-conserved Niddm1i of the GK rat. *Genetics* **174**, 1565-1572 (2006).
311 15. Clee, S.M., *et al.* Positional cloning of Sorcs1, a type 2 diabetes quantitative trait locus. *Nat*
312 *Genet* **38**, 688-693 (2006).
313 16. Kebede, M.A., *et al.* SORCS1 is necessary for normal insulin secretory granule biogenesis in
314 metabolically stressed beta cells. *J Clin Invest* **124**, 4240-4256 (2014).
315 17. Hermey, G., Sjogaard, S.S., Petersen, C.M., Nykjaer, A. & Gliemann, J. Tumour necrosis factor
316 alpha-converting enzyme mediates ectodomain shedding of Vps10p-domain receptor family
317 members. *Biochem J* **395**, 285-293 (2006).
318 18. Hermey, G., *et al.* Characterization of sorCS1, an alternatively spliced receptor with completely
319 different cytoplasmic domains that mediate different trafficking in cells. *J Biol Chem* **278**,
320 7390-7396 (2003).

321 19. Graae, A.S.*, et al.* ADAMTS9 Regulates Skeletal Muscle Insulin Sensitivity Through
322 Extracellular Matrix Alterations. *Diabetes* **68**, 502-514 (2019).
323 20. Ayala, J.E.*, et al.* Standard operating procedures for describing and performing metabolic tests
324 of glucose homeostasis in mice. *Dis Model Mech* **3**, 525-534 (2010).
325 21. Vaegter, C.B.*, et al.* Sortilin associates with Trk receptors to enhance anterograde transport and
326 neurotrophin signaling. *Nat Neurosci* **14**, 54-61 (2011).
327 22. Glerup, S.*, et al.* SorCS2 is required for BDNF-dependent plasticity in the hippocampus. *Mol*
328 *Psychiatry* **21**, 1740-1751 (2016).
329 23. Martinez Molina, D.*, et al.* Monitoring drug target engagement in cells and tissues using the
330 cellular thermal shift assay. *Science* **341**, 84-87 (2013).
331 24. Januliene, D.*, et al.* Hidden Twins: SorCS Neuroreceptors Form Stable Dimers. *J Mol Biol* **429**,
332 2907-2917 (2017).
333 25. Kerppola, T.K. Design and implementation of bimolecular fluorescence complementation
334 (BiFC) assays for the visualization of protein interactions in living cells. *Nat Protoc* **1**, 1278-
335 1286 (2006).
336 26. Nakayama, K. Furin: a mammalian subtilisin/Kex2p-like endoprotease involved in processing
337 of a wide variety of precursor proteins. *Biochem J* **327 (Pt 3)**, 625-635 (1997).
338 27. Breining, P.*, et al.* Assessment of changes in real time net glucose uptake in adherent cell
339 models upon acute stimulation. *Bio-protocol. bio-protocol.org/prep1478.* (2021).
340 28. Leloup, N., Chataigner, L.M.P. & Janssen, B.J.C. Structural insights into SorCS2-Nerve
341 Growth Factor complex formation. *Nat Commun* **9**, 2979 (2018).
342 29. Waterhouse, A.*, et al.* SWISS-MODEL: homology modelling of protein structures and
343 complexes. *Nucleic Acids Res* **46**, W296-W303 (2018).
344